

# Measurement of foil thickness in transmission electron microscopy

ZHENPENG PAN\*, C. K. L. DAVIES, R. N. STEVENS

*Department of Materials, Queen Mary and Westfield College, Mile End Road, London E14NS, UK*

Methods for the measurement of the thickness of thin-foil specimens used in transmission electron microscopy are either difficult to carry out or have been subject to criticism. In particular, the contamination spot method is said to overestimate the thickness because the region of rapidly changing contrast marking the apparent edge of the spot is not on the foil surface but is on a broad contamination deposit whose thickness is changing much more slowly. A new method for measuring foil thickness is proposed, based on contamination deposits on the foil surfaces. The problems of the contamination spot method, in which the deposit is of circular form, are avoided by using one of the condenser lenses to focus the electron beam in a thin line on the foil during deposition. Adequate contrast can be obtained with a line whose width is one-third to one-fifth of the foil thickness and having a height equal to or less than its width. The error, being a fraction of the line width, is then very small. After rotation of the foil, the lines separate into two and the corresponding edges of the lines provide distinct features whose separation can be measured to determine thickness. The axis of rotation, perpendicular to which the separation of the lines has to be measured to calculate foil thickness, is determined by depositing two contamination lines at right angles. The method allows a number of measurements of thickness covering a relatively large area of foil to be made per contamination experiment. Near the edge of the foil, the upper and lower lines of contamination can join around the foil edge to form a U shape which can be used to measure thickness profile of the foil right up to the edge.

## 1. Introduction

A knowledge of the thickness of the thin foils used as specimens in transmission electron microscopy is required for many purposes, including the determination of such quantities as dislocation density and the volume fraction of precipitated phases. Methods for the measurement of the thicknesses of thin foils in transmission electron microscopy include the spot contamination method [1], the convergent beam diffraction method [2] and methods based on characteristic X-ray emission [3] and continuous X-ray emission [4]. Of these, the convergent beam method is the most basic but it is difficult to carry out and the subsequent calculations are complicated [5]. The contamination spot method is, on the other hand, very simple in principle and straightforward in use. It involves focusing the electron beam into an intense circular spot on the specimen and, without a cold trap in operation, allowing time for the build up of carbon contamination at both the point where the beam impinges on the upper surface of the foil and at the point where the beam emerges from the lower surface. Tilting the foil through a known angle,  $\phi$ , causes the images of the upper and lower contamination spots to separate and measurement of this separation,  $r$ , enables the foil thickness,  $t$ , to be simply calculated. If the beam is perpendicular to the foil surface during depos-

ition then the thickness is given by

$$t = r/(M \sin \phi) \quad (1)$$

where the distance  $r$  is measured in an image at a magnification of  $M$ . This is illustrated in Fig. 1. If the spots are deposited when the beam is at an angle  $\psi$  to the foil normal, the thickness is calculated from

$$t = r \cos \psi / (M \sin \phi) \quad (2)$$

where it is assumed that both  $\phi$  and  $\psi$  are positive.

However, doubt has been cast on the accuracy of the method by a number of workers [6–8]. Stenton *et al.* [8] carried out contamination spot determinations of the thicknesses of evaporated thin films and compared the results with measurements using optical interferometry. It was found that the contamination spot method overestimated the film thickness by ~50% to ~200%. Although comparison with the convergent beam technique by Kouh and Hall [9] suggested rather lower overestimates by the contamination spot method (~15%), the evidence that it involves a systematic error is convincing.

An explanation of this error has been suggested by Rae *et al.* [7]. They reported that beneath the sharp cones that are usually observed on the specimen there are faint and relatively broad contamination deposits whose thickness changes much more slowly than that

\* Permanent address: Guangdong Mechanical College, Guangzhou, 510643 People's Republic of China.

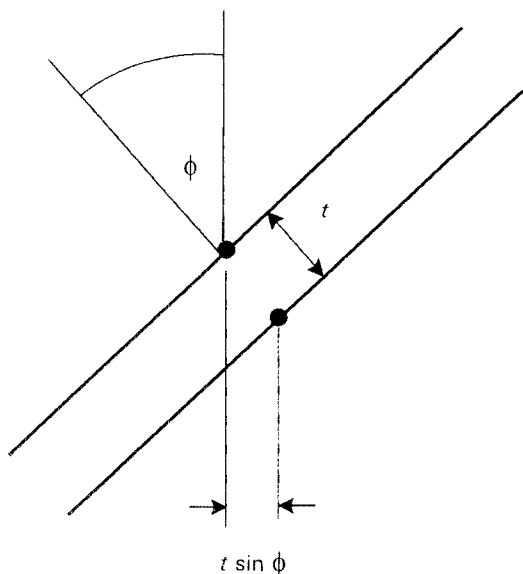


Figure 1 Illustrating the principle of the measurement of foil thickness using the contamination spot method. Tilting the foil through an angle  $\phi$  causes the separation of the projected images of spots on the upper and lower surfaces allowing  $t$  to be determined.

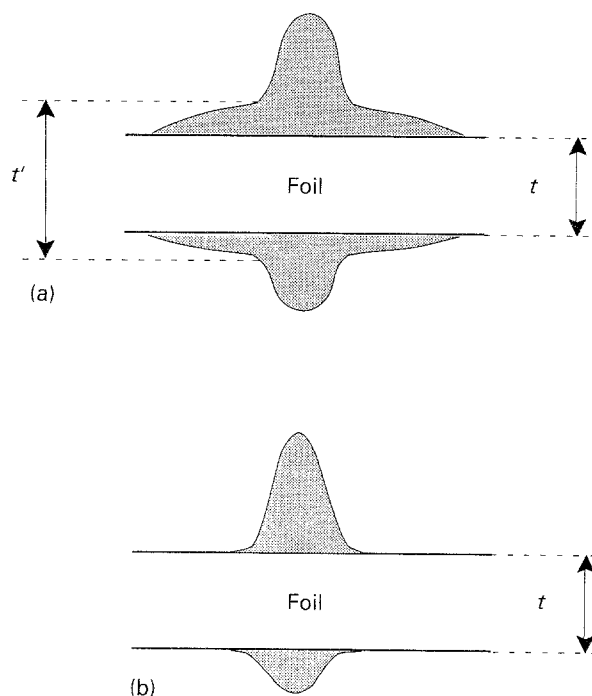


Figure 2 The real (a) and assumed (b) configurations of the contamination deposit on the foil according to Rae *et al.* [7]. The "witches hat" configuration in (a) implies that the apparent foil thickness,  $t'$ , is greater than the true thickness,  $t$ , because of the broad base of the deposit.

of the central spot. The overall configuration is that of a "witch's hat" and is illustrated in Fig. 2a. It is generally assumed that the base of the sharp cones is on the foil surface as in Fig. 2b and the reason for the overestimation is easy to see. Rae *et al.* [7] also point out that the images of the contamination spots are complex and it is far from obvious between which features in the image measurements of  $r$  are to be made, introducing further errors.

## 2. The contamination line method

The simplicity and convenience of the contamination spot method make it worthwhile attempting to eliminate or reduce the problems described above. To form the spot, the electron beam is normally focused to give the smallest possible circle on the foil surface. However, in the Jeol 100CX microscope, the beam can also be focused to one of two possible thin lines at right angles (of length-to-width ratio of  $\sim 30:1$ ) or to one of two perpendicular lenticular shapes using condenser lens 2. Exposure using the line configuration of the electron beam gave well-defined lines of contamination with sharply pointed ends on both surfaces of the foil. The length and width of the contamination lines increased with exposure time. Adequate contrast could be obtained with exposures of a few minutes with the smallest spot size set (number 4) with condenser lens 1 and a condenser aperture of  $100\ \mu\text{m}$  diameter (or occasionally  $400\ \mu\text{m}$  or  $200\ \mu\text{m}$  diameter). This resulted in lines typically  $\sim 60\ \text{nm}$  wide. Measurement of the images of the lines after tilting implied that the height of the deposit above the foil is similar to or less than the width.

Tilting the foil caused the images of the upper and lower contamination lines to separate as shown in the example shown in Fig. 3. If the lines are parallel to the axis of rotation of the foil, then Equation 1 can be used to calculate the foil thickness using measurements of the separation,  $r$ , of corresponding edges. The separation can be measured at an arbitrary number of points along the line. A pair of contamination lines

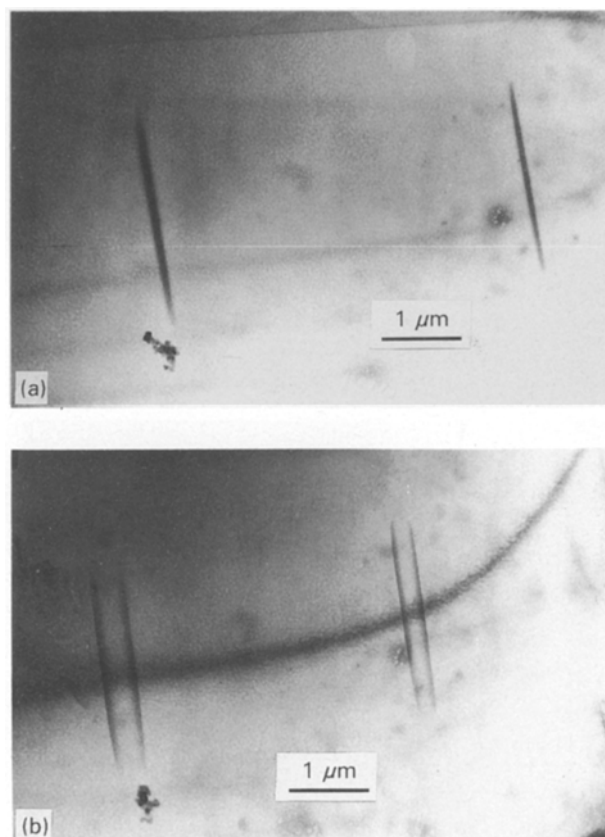


Figure 3 Contamination lines on the surfaces of an Al/2.75% Li (by mass) alloy (a) with zero rotation, and (b) with a rotation of  $45^\circ$ .

therefore allows a series of values of thickness to be measured along a given direction, whereas the spot method measures the thickness only at a single point.

Because the width of the deposited line and its height are low, the influence of the broader and thinner contamination layer beneath the line is minimal. In most cases the line width (and hence the height) is only a fraction of the foil thickness, typically about one-quarter. Any error will be less than the height of the deposit and hence less than the line width. The errors in this method are likely to be very small compared to the errors reported by Stenton *et al.* [9] for the spot method. The edges of the lines also provide unambiguous features in the image between which measurements can be made. If the height of the contamination lines is less than the width, the foil can be tilted through  $45^\circ$  or more without a spurious edge appearing due to the top of the deposit overlapping the edge on the foil surface. As already noted, the images of contamination spots after tilting are more complex and there is often considerable difficulty in picking out the features between which to make measurements [7].

The rotation axis will not, in general, be parallel to the contamination lines and when this is the case  $r$  has to be measured, not perpendicular to the lines, but perpendicular to the axis about which the foil is rotated. It is difficult to arrange for the rotation axis to be parallel to the contamination lines and it is necessary to determine its direction relative to the lines if

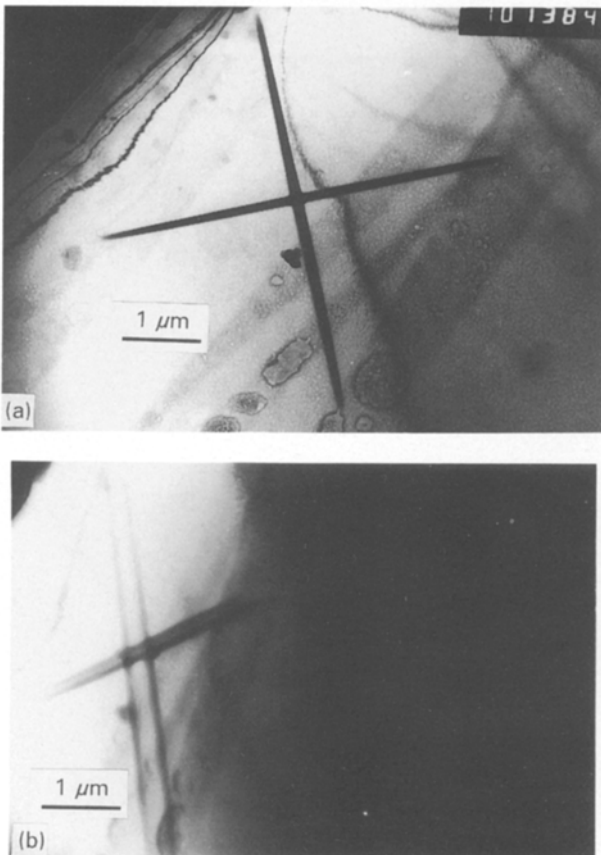


Figure 4 Two contamination lines on the surfaces of a thin foil of an Al/2.75% Li (by mass) alloy at right angles (a) with zero rotation, and (b) with  $55^\circ$  rotation.

the thickness is to be measured and the method is to be of general use. This can be done by using two lines crossing at right angles as shown in Fig. 4. After rotation of the foil about an axis making an arbitrary angle with one of the lines, the two pairs of initially perpendicular lines will no longer be perpendicular and will have different separations. The first method uses the apparent angle between the lines after rotation. The geometry is illustrated in Fig. 5. The angles between the axis and each of the two lines before rotation are  $\alpha$  and  $\beta$  respectively ( $\beta = \pi/2 - \alpha$ ), while after a rotation  $\phi$  these change to  $\alpha'$  and  $\beta'$ . We have

$$\tan \alpha' = \tan \alpha \cos \phi \quad (3)$$

and

$$\tan \beta' = \tan \beta \cos \phi = \cot \alpha \cos \phi \quad (4)$$

If  $\alpha'$  or  $\beta'$  are known, a line parallel to the rotation axis can be drawn on a photograph and the separation,  $r$ , perpendicular to this axis can be measured for use in Equations 1 or 2. The most convenient way to do this is to note that the angle,  $\lambda$ , between the contamination line and the direction in which  $r$  is to be measured is given by  $\lambda = \pi/2 - \beta'$ , as can be seen in Fig. 6. Clearly  $\alpha'$  and  $\beta'$  can be found if  $\alpha$  is known. For a given accelerating voltage and setting of condenser lens 1, the angle  $\alpha$  is fixed and can be considered as an instrument constant. It can be determined by a calibration experiment using two perpendicular contamination lines. The angle,  $\gamma'$  ( $=\alpha' + \beta'$ ) between the two lines is measured after rotation by a given large angle,  $\phi$ . Equations 3 and 4 lead to

$$\tan \alpha = \frac{1}{2\cos \phi} [\sin^2 \phi \tan \gamma' + (\sin^4 \phi \tan^2 \gamma' - 4 \cos^2 \phi)^{1/2}] \quad (5)$$

The same formula with a minus sign replacing the plus sign in front of the term in parentheses gives the value of  $\tan \beta$ . Inspection is sufficient to clear up any ambiguities. The rotation axis must lie between the lines making an acute angle with each other and must lie closer to the pair of lines with the greater separation.

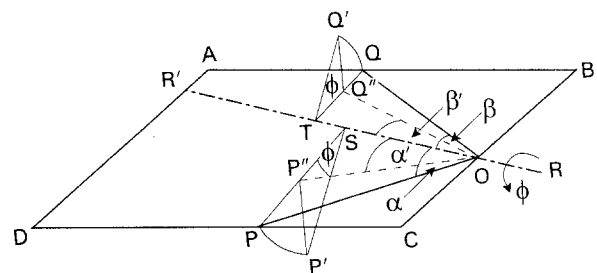


Figure 5 The geometry of the change in angle between two contamination lines with rotation. ABCD is the plane of the foil before rotation, RR' is the rotation axis and PO and OQ are the perpendicular contamination lines. The points P and Q are rotated through an angle  $\phi$  to P' and Q', respectively, and these project to points P'' and Q'' on the original plane. Hence the images of the lines after rotation are P''O and Q''O making angles  $\alpha'$  and  $\beta'$  with the rotation axis.

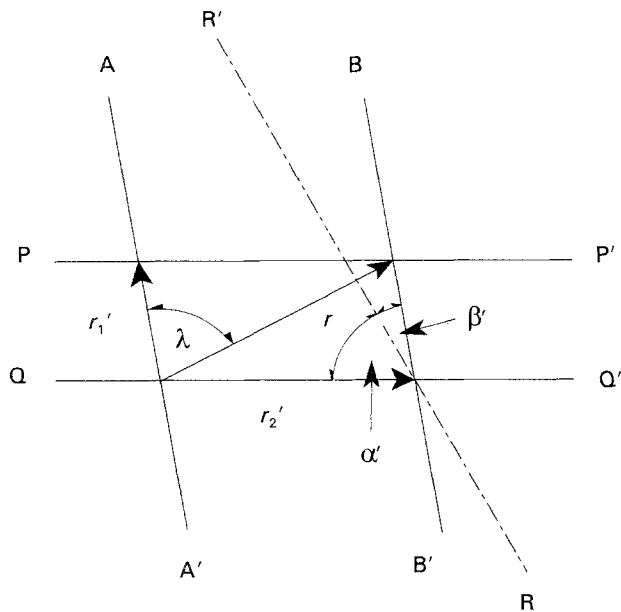


Figure 6 The graphical method of determining the angles  $\alpha'$  and  $\beta'$  and the separation,  $r$ . The separation  $r_1'$  of the first pair of lines is measured parallel to the second pair and similarly for  $r_2'$ . The parallelogram is drawn with  $r_1'$  parallel to the second set and  $r_2'$  parallel to the first. The separation,  $r$ , is then equal to the diagonal of the parallelogram. The rotation axis,  $RR'$ , can thus be drawn perpendicular to the diagonal of the parallelogram. The angle,  $\lambda$ , between the direction of  $r$  and the contamination line is given by  $\lambda = \pi/2 - \beta'$ .

An alternative, graphical method is to construct the parallelogram shown in Fig. 6. This allows both the value of  $\alpha$  and the value of the separation,  $r$ , to be measured using the same construction. The separations,  $r_1'$  and  $r_2'$  of the two pairs of lines are measured near the intersection point. Here  $r_1'$  is the separation of the first pair of lines measured in the direction of the second pair and  $r_2'$  the separation of the second measured in the direction of the first. The parallelogram in Fig. 6 has sides  $r_1'$  and  $r_2'$  parallel to the directions in which they are measured. The diagonal of the parallelogram is the direction in which the measurements have to be made (i.e. it is perpendicular to the axis of rotation). It can be seen that both  $r$  and  $\alpha'$  and hence  $\alpha$  can be measured from this construction.

Once  $\alpha$  is known with reasonable accuracy it can be used to locate the rotation axis using Equation 3 or 4 and thereafter only single contamination lines need be used for thickness determinations. On our instrument (Jeol JEM 100CX) at 100 kV and spot size 4,  $\alpha$  is  $83^\circ$  ( $\beta = 7^\circ$ ) and a  $45^\circ$  rotation gives  $\alpha' = 80.15^\circ$ ,  $\beta' = 4.95^\circ$  and  $\lambda = 85.05^\circ$ .

### 3. Measurements at the foil edge

Having focused the beam to a thin line, it is possible for the tip of the line to project to or beyond the edge of the foil. The contamination deposit then joins up around the foil edge to form an elongated U shape, as shown in Fig. 7. Rotation of the foil then allows foil thickness to be determined right up to the edge and the profile of the foil edge found, something which is

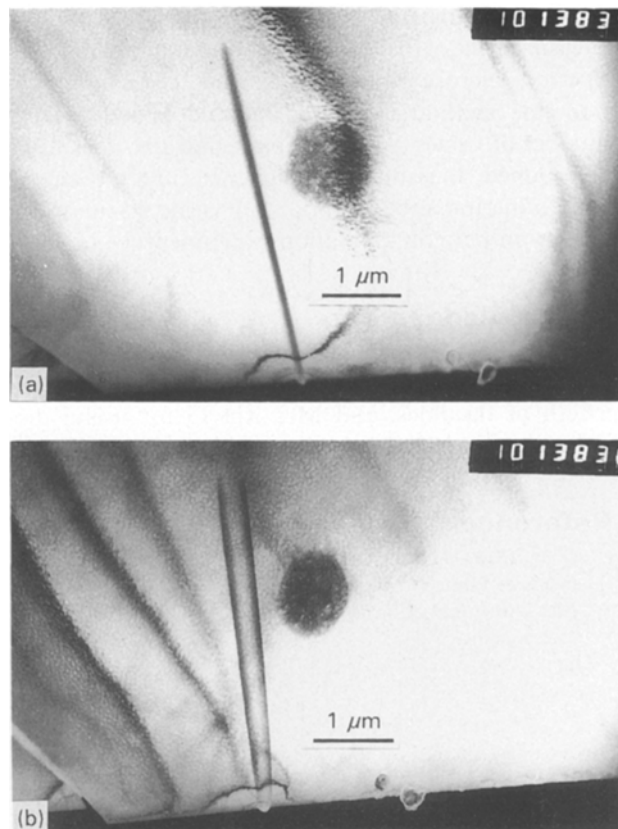


Figure 7 A U-shaped deposit going right round the edge of the foil in an Al/2.75% Li (by mass) alloy foil, (a) with zero rotation, and (b) with  $45^\circ$  rotation.

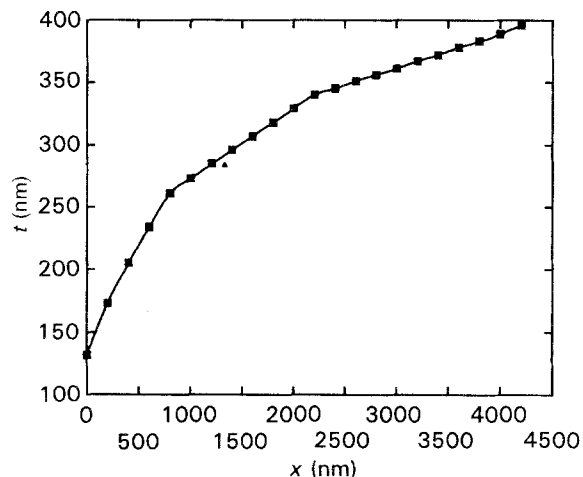


Figure 8 The foil profile up to the edge as obtained from Fig. 7. The foil thickness is  $t$  and  $x$  is the distance from the edge along the contamination line. Note the difference in scales for  $t$  and  $x$ .

particularly difficult with other methods. Fig. 8 shows the calculated profile of the foil shown in Fig. 7 and illustrates how much data one experiment of this kind can yield.

Greater accuracy could be achieved if smaller beam spot sizes and smaller condenser apertures could be used to produce narrower lines (and hence lines of lower height) provided that sufficient contrast could be obtained. It would be useful and more convenient if the lines could be deposited accurately parallel to the rotation axis.

#### 4. Conclusions

Measurement of the thickness of thin-foil transmission electron microscope specimens using the contamination line method is convenient and allows a large number of values along two perpendicular lines to be determined. It is of much higher accuracy than the contamination spot method and yields far more information per contamination experiment.

#### Acknowledgements

We thank Mr Qinglong Yuan for help with the use of the condenser aperture to give optimum width and length of the lines, and Mrs Xia Li for useful discussions about the method in general.

#### References

1. G. W. LORIMER, G. CLIFF and J. N. CLARK, in "Developments in Electron Microscopy and Analysis" edited by D. L. Misell (Institute of Physics, Bristol, 1976) p. 153.

2. P. M. KELLY, A. JOSTONS, R. G. BLAKE and J. G. NAPIER, *Phys. Status solidi (a)* **31** (1975) 771.
3. G. LOVE, M. G. C. COX and V. D. SCOTT, in "Developments in Electron Microscopy and Analysis" edited by D. L. Misell (Institute of Physics, Bristol, 1976) p. 347.
4. W. S. MILLER and V. D. SCOTT, *Met. Sci. J.* **12** (1978) 95.
5. V. D. SCOTT and G. LOVE, *Mater. Sci. Technol.* **3** (1987) 600.
6. A. D. ROMIG and M. J. CARR, "Analytical Electron Microscopy—1984" (San Francisco Press, San Francisco, 1984) p. 111.
7. D. A. RAE, V. D. SCOTT and G. LOVE, in "Quantitative Microanalysis with High Spatial Resolution" edited by G. W. Lorimer (The Metals Society, London, 1981) p. 57.
8. N. STENTON, M. R. NOTIS, J. I. GOLDSTEIN and D. B. WILLIAMS, *ibid.* p. 35.
9. Y. KOUH and E. L. HALL, General Electric Technical Information, Series 7 Report no. 82 CRD (1982) p. 156.

*Received 26 August  
and accepted 14 September 1993*